arXiv:1402.5543v1 [cond-mat.str-el] 22 Feb 2014

LDA+DMFT Approach to Magnetocrystalline Anisotropy of Strong Magnets

Jian-Xin Zhu,[1,*] Marc Janoschek,[1] Richard Rosenberg,[2] Filip Ronning,[1]
Joe D. Thompson,[1] M. A. Torrez,[1] Eric D. Bauer,[1] and Cristian D. Batista[1,†]

[1] *Los Alamos National Laboratory, Los Alamos, New Mexico 87545, USA*
[2] *Advanced Photon Source, Argonne National Laboratory, Argonne, Illinois 60439, USA*

The new challenges posed by the need of finding strong rare-earth free magnets demand methods that can predict magnetization and magnetocrystalline anisotropy energy (MAE). We argue that correlated electron effects, which are normally underestimated in band structure calculations, play a crucial role in the development of the orbital component of the magnetic moments. Because magnetic anisotropy arises from this orbital component, the ability to include correlation effects has profound consequences on our predictive power of the MAE of strong magnets. Here we show that incorporating the local effects of electronic correlations with dynamical mean-field theory provides reliable estimates of the orbital moment, the mass enhancement and the MAE of YCo_5.

PACS numbers: 71.15.Mb, 71.15.Rf, 71.27.+a, 75.30.Gw

I. INTRODUCTION

Magnets play a central role in different types of devices and motors, which are at the heart of modern technology. There is an increasing need of permanent magnetic materials for energy conversion and power generation [1]. Magnetocrystalline anisotropy (MA) is one of the most important properties of permanent magnets [2]. Large MA is achieved in existing strong magnets by using rare-earth-transition metal intermetallic compounds, such as $SmCo_5$ and $Nd_2Fe_{14}B$, which are of direct technological use. However, the shortage of rare-earth elements has triggered the search for rare-earth-free magnetic materials harnessing sources of magnetic anisotropy other than that provided by the rare-earth components [1]. In order to guide this search, it is necessary to develop theoretical methods that can estimate the magnetocrystalline anisotropy energy (MAE) of 3*d*, 4*d* and 5*d* transition metals, which are the natural candidates for replacing rare-earth elements.

The contribution of itinerant ferromagnetic electrons to MA arises from the spin-orbit (SO) interaction that couples the spin and orbital components of the magnetic moments. MA results from the orbital component of the moment, which is sensitive to the lattice anisotropy. While a band picture may provide a MAE of the right order of magnitude for certain transition metal ferromagnets [3, 4], accurate electronic structure calculations of the MAE of 3*d* metals, such as Fe, Co and Ni, give numbers that are in disagreement with experiment [5]. Moreover, the wrong easy-axis is obtained for Co and Ni. This failure has been attributed to either the omission of the orbital correlation induced by the intra-atomic Coulomb interaction between electrons [6] or the limitation of band structure calculations for calculating energy differences of the order of 0.1 meV [5].

YCo_5 has one of the largest MAEs among ferromagnets that do not include *f*-electron (actinide or lanthanide) ions. The MAE is more than 50 times larger than in the pure cobalt metal. Like $SmCo_5$, it has an easy-axis parallel to the *c*-axis of its hexagonal lattice structure. The primitive unit cell contains six atoms with two different cobalt sites, Co_I (2c) and Co_{II} (3g) [7]. Neutron scattering experiments by Schweizer *et al.* have reported unusually large orbital moments on these Co sites [8]: m_{orb}(Co-2c)=0.46μ_B and m_{orb}(Co-3g)=0.28μ_B. However, our x-ray magnetic circular dichroism (XMCD) measurements indicate that the average orbital moment of Co is 0.2 μ_B, in better agreement with the value of 0.25 μ_B reported by Heidemann *et al.* [9]. These measurements suggest that the rather large orbital magnetic moments of the Co atoms are partially responsible for the strong MAE of YCo_5. Consequently, reliable estimates of the MAE require an accurate calculation of these orbital moments. This is not only true for YCo_5, but also for any other strong magnet based on transition metals. We will then use YCo_5 as a prototype compound for developing and testing methods for calculating the orbital moments and the MAE of strong magnets.

Nordström *et al.* [7] have applied the force theorem to compute the MAE of YCo_5 from first-principles calculations. It was found that, in the absence of atomic orbital correlation, the MAE is too small and it even has the incorrect sign, in agreement with Ref. [5]. After including the orbital polarization (OP) scheme suggested by Brooks [10, 11], they were able to obtain a MAE that has the correct sign. However, the MAE value of about 50μRyd, when extrapolated to the infinitesimal grid in the momentum space although, is still too small in comparison with the experimental value of 292 μRyd [12]. A similar improvement is obtained for estimations of the orbital magnetic moments of both Co sites. In absence of orbital correlation, the result is m_{orb}(Co-2c)=0.1μ_B and m_{orb}(Co-3g)=0.13μ_B [13], while the inclusion of OP leads to m_{orb}(Co-2c)=0.27μ_B and m_{orb}(Co-3g)=0.20μ_B [7].

The OP scheme is taken from the theory of open shell atoms within the Russel-Saunders coupling. The

* jxzhu@lanl.gov
† cdb@lanl.gov

ground state energy gain, that is obtained by maximizing the orbital angular momentum L, is approximated by $E_{\rm OP} = -BL^2/2$, where B is the Racah parameter for d sates. This effect is just a consequence of the Coulomb interaction between d-electrons that occupy the same ion and it must influence the final value of the orbital magnetic moment and the MAE. However, it is well known that the electron-electron Coulomb interaction also affects the band states by developing inter-atomic correlations (electrons tend to avoid each other). Therefore, it is reasonable to expect that this second consequence of the Coulomb interaction will also affect the magnitude of the orbital magnetic moment and the MAE. Here we propose a method for including these additional correlations.

II. ROLE OF COULOMB INTERACTION ON LOCAL MOMENT FORMATION

The effect of electron-electron interaction is to reduce the bandwidth of the quasi-particles and produce an incoherent component in their spectral weight. The most dramatic effect of this Coulomb repulsion is the emergence of Mott insulators in half-filled bands via localization of individual electrons in their atomic orbitals. The electronic localization is accompanied by the formation of a local magnetic moment, whose spin and orbital components can be of the order of a Bohr magneton (μ_B) [14]. It is clear that Coulomb interaction cannot localize the electronic charge away from half-filling. However, the band narrowing effect can be interpreted as a tendency towards localization that favors local moment formation. This simple reasoning suggest that the inclusion of electronic correlations should lead to more realistic values of the effective mass of the quasiparticles, orbital magnetic moments and MAE.

Standard LDA calculations lead to orbital magnetic moments of order $0.1\mu_B$. This result can be understood in the following way. The typical bandwidths, W, of $3d$ metals like Fe or Co are of the order of a few eV. The SO interaction is of order $\lambda \simeq$0.1eV. In the absence of SO coupling, the ground state has zero orbital angular momentum, even if it has a net spin magnetization, because single-particle states with opposite values of the orbital magnetic moment are degenerate and therefore equally occupied. A finite SO coupling term splits states with opposite values of orbital moment by an amount that is of order λ. This observation implies that only the electronic states that are within a distance λ from the Fermi level contribute to orbital polarization. The fraction of electrons occupying these states is of order $\lambda/W \simeq 0.1$. Because the maximum possible value of the orbital moment per atom is of order $1\mu_B$, this rough estimate indicates that $m_{\rm orb} \lesssim 0.1\ \mu_B$ in agreement with previous results from standard band structure calculations [7]. However, as pointed out in the introduction, the orbital magnetic moment of strong magnets, such as YCo_5, can be higher than this rough estimate.

It is natural to assume that the discrepancy arises from the effects of rather strong intra and inter-atomic electronic correlations induced by the Coulomb interaction. The improvement that is obtained after including the intra-atomic OP effect provides empirical support for this assumption. However, the most basic and general argument in favor of this assumption is that intra-atomic Coulomb repulsion favors local moment formation by suppressing double occupancy of single atomic orbitals. The importance of correlation effects on the magnetic anisotropy of Fe and Ni was already recognized more than ten years ago by Yang *et al.* [15]. This problem is now timely because of the increasing need of finding strong magnets that are free of rare earth elements. Therefore, it is crucial to propose new methods that can incorporate the subtle effects of correlations in solids (the OP effect that we discussed above is already captured at the level of single-atom physics). For this purpose we propose a method based on the combination of the dynamical mean-field theory (DMFT) and the LDA [16]. A similar approach has been successfully applied to the calculation of neutron magnetic form factors for actinides by applying an external magnetic field [17], as well as the bulk and surface quasiparticle spectra for Fe, Co, and Ni metals [18]. The basic idea is to treat each Co ion as an effective impurity that is embedded into the bath generated by the rest of the ions. The single-ion interactions (including the OP) are captured by the single-impurity Hamiltonian. The correlations developed via the interplay between the single-ion terms and the interaction with the bath (solid) are captured by a self-consistent treatment of the full Hamiltonian that we describe in the next section.

III. LOCAL DENSITY APPROXIMATION PLUS DYNAMICAL MEAN-FIELD THEORY

To study the role of electronic correlations on the orbital moment of the magnetic $3d$ ions by combining the LDA with dynamical mean-field theory (LDA+DMFT) [16] we start with a generalized many-body Hamiltonian:

$$\hat{H} = \sum_{\mathbf{k},lm_l\sigma,l'm'_l\sigma'} [H^{(0)}_{\mathbf{k}}]_{lm_l\sigma,l'm'_l\sigma'} c^{\dagger}_{\mathbf{k}lm_l\sigma} c_{\mathbf{k}l'm'_l\sigma'} + \frac{1}{2} \sum_{,l=2(3),m_lm'_l,\ m''_lm'''_l\sigma\sigma'} V_{m_lm'_lm''_lm'''_l} c^{\dagger}_{ilm_l\sigma} c^{\dagger}_{ilm'_l\sigma'} c_{ilm'''_l\sigma'} c_{ilm''_l\sigma} \quad (1)$$

Here $\mathbf{k}$ is a wave vector of the Brillouin-zone, i is a lattice site index for atoms with correlated orbitals, l is the orbital angular momentum, $m_l = -l, -l+1, \ldots, l-1, l$, and σ is the spin projection quantum number. The field operator $c^{\dagger}_{ilm_l\sigma}$ ($c_{ilm_l\sigma}$) creates (annihilates) an electron with spin σ and orbital indices (lm_l) at site i, while $c^{\dagger}_{\mathbf{k}lm_l\sigma}$ ($c_{\mathbf{k}lm_l\sigma}$) is the corresponding operator in momentum space. The first term of $\hat{H}$ contains the single-particle

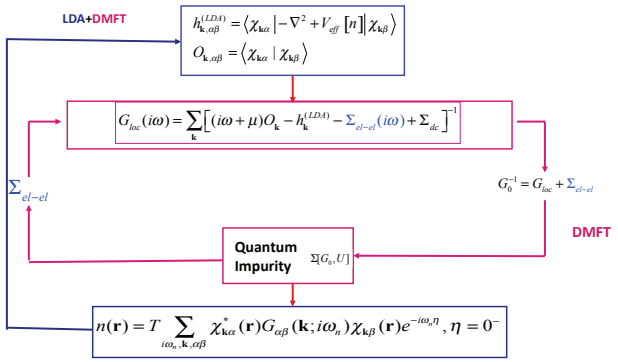
LDA+DMFT
$h^{(LDA)}_{\mathbf{k}\alpha\beta} = \langle \chi_{\mathbf{k}\alpha} | -\nabla^2 + V_{eff}[n] | \chi_{\mathbf{k}\beta} \rangle$
$O_{\mathbf{k},\alpha\beta} = \langle \chi_{\mathbf{k}\alpha} | \chi_{\mathbf{k}\beta} \rangle$
$G_{loc}(i\omega) = \sum_{\mathbf{k}} [(i\omega+\mu)O_{\mathbf{k}} - h^{(LDA)}_{\mathbf{k}} - \Sigma_{el-el}(i\omega) + \Sigma_{dc}]^{-1}$
Σ_{el-el}
$G_0^{-1} = G_{loc}^{-1} + \Sigma_{el-el}$
DMFT
Quantum Impurity
$\Sigma[G_0, U]$
$n(\mathbf{r}) = T \sum_{i\omega_n, \mathbf{k}, \alpha\beta} \chi^*_{\mathbf{k}\alpha}(\mathbf{r}) G_{\alpha\beta}(\mathbf{k}; i\omega_n) \chi_{\mathbf{k}\beta}(\mathbf{r}) e^{-i\omega_n \eta}, \eta = 0^-$

FIG. 1. Schematic description of the DMFT+LDA approach.

contribution, which is determined by solving the Kohn-Sham quasi-particle equations [19] within LDA. We note that the SO coupling can be included in a second variational way in the LDA Hamiltonian. In the second term of $\hat{H}$ we restrict the Coulomb repulsion to the correlated orbitals (e.g., open shell Co $3d$ orbitals ($l = 2$) or Ce $4f$ orbitals ($l = 3$)) to reduce the complexity of the problem [16]. The Coulomb matrix elements are obtained from atomic physics:

$$V_{m_l m_l' m_l'' m_l'''} = \sum_{k(even)=0}^{2l} a_k(m_l, m_l', m_l'', m_l''') F^k \ , \quad (2)$$

where F^k and a_k are the Slater integrals and the corresponding expansion coefficients [20]. For solids, we identify the atomic Slater integral F^0 with the screened effective Coulomb interaction parameter U of the correlated orbitals. As a common practice, higher order Slater integrals are reduced by 20% from the atomic Hartree-Fock calculations due to screening effects [21].

Within DMFT, the lattice problem of Eq. (1) is mapped onto a multi-orbital quantum single impurity problem subject to the self-consistency condition (see Fig. 1):

$$\hat{\mathcal{G}}^{-1}(i\omega_n) = \hat{G}^{-1}_{\rm loc}(i\omega_n) + \hat{\Sigma}(i\omega_n) \ . \quad (3)$$

Here $\hat{\mathcal{G}}(i\omega_n)$ is the Weiss function, $\hat{\Sigma}(i\omega_n)$ is a $\mathbf{k}$-independent self-energy, and the local Green's function is defined as $\hat{G}_{\rm loc}(i\omega_n) = \sum_{\mathbf{k}} \hat{G}_{\mathbf{k}}(i\omega_n)/N$, where the lattice Green's function reads

$$\hat{G}_{\mathbf{k}}(i\omega_n) = [(i\omega_n + \mu)\hat{I} - \hat{H}^0(\mathbf{k}) - \hat{\Sigma}(i\omega_n)]^{-1} \ . \quad (4)$$

$\hat{I}$ is the identity matrix in the complete tight-binding basis and μ is the chemical potential. Because we have added the on-site Coulomb terms to the correlated valence orbitals only, it is evident that the self-energy $\hat{\Sigma}$ matrix has nonzero elements only within the 10×10 d-d block for the case of valence d-orbitals, or the 14×14 f-f block for the case of valence f-orbitals. This self-energy matrix is a function of the Matsubara frequency: $\Sigma^{dd(ff)}_{m_l\sigma,m_l'\sigma'}(i\omega_n)$. Correspondingly, the local Green's function for the correlated orbitals has the same structure $G^{dd(ff)}_{{\rm loc},m_l\sigma,m_l'\sigma'}(i\omega_n)$. We assume that the dominant contributions to the spin and orbital components of the magnetic moments come from the correlated orbitals (Co $3d$-orbitals for the case of YCo_5). After obtaining the local Green's function for the correlated orbitals through the full self-consistency, we can evaluate the spin and orbital moments by computing $M_s = \sum_{m_l\sigma} \sigma \rho_{m_l\sigma,m_l\sigma}$ and $M_{orb} = \sum_{m_l\sigma} m_l \rho_{m_l\sigma,m_l\sigma}$, respectively, in the spherical harmonics basis. Here the density matrix is related to the local Green's function as

$$\hat{\rho} = \hat{G}^{dd(ff)}_{loc}(\tau \to 0^-) = \frac{1}{\beta} \sum_{i\omega_n} \hat{G}^{dd(ff)}_{loc}(i\omega_n) e^{-i\omega_n 0^-} \ , \quad (5)$$

where $\beta = 1/k_B T$, with k_B and T the Boltzmann constant and temperature, respectively.

In earlier applications of the LDA+DMFT method, it is common use to rotate the local Green's function and the corresponding self-energy into a basis in which the diagonal matrix elements are dominant in order to neglect the off-diagonal elements. For example, for actinide based materials, the correlated $5f$ orbitals are rotated into the J-J basis because of the dominant SO coupling [22, 23]. In contrast, SO coupling is subdominant for d-electron materials, like transition metal oxides, and the matrix is diagonal in the crystal field basis when the SO coupling is neglected [24–27]. However, the off-diagonal matrix elements cannot be neglected if our goal is to compute the MAE (the SO coupling must be included to obtain a finite MAE and the orbital magnetic moment has only off-diagonal contributions in this basis). This situation requires a further development of quantum impurity solvers to meet this challenge and similar challenges posed by other correlated electron materials, such as the inclusion of crystal field terms in $4f$ and $5f$ compounds.

IV. COMPUTATIONAL RESULTS

Here we use the spin-polarized T-matrix fluctuation-exchange approximation technique (SPTF) [28] to solve the effective quantum impurity problem. In this formalism, the self-energy includes Hartree and Fock diagrams with the bare interaction replaced by the T matrix and particle-hole contributions with the bare interaction replaced by the particle-hole potential fluctuation matrix. The T matrix and the particle-hole potential fluctuation matrix are in turn expressed in terms of particle-particle and particle-hole susceptibilities. We use the charge self-consistent LDA+DMFT(SPTF) approach as implemented in an electronic structure code based on a full-potential linear muffin-tin orbital method (LMTO) [29, 30]. The LMTO basis sets contain a triple basis for s and p states and a double basis for the d orbitals of YCo_5. The basis of the valence electrons is

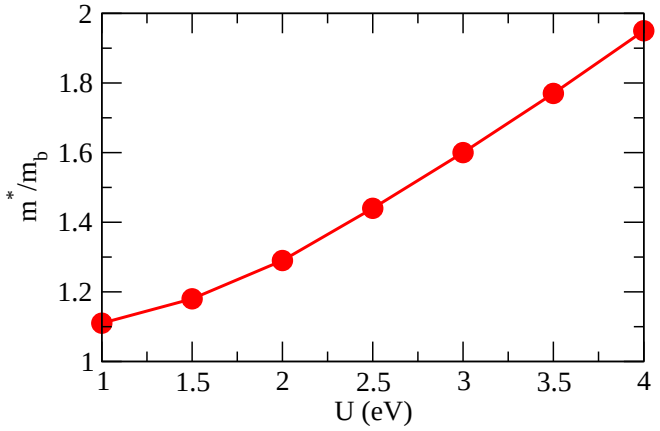

FIG. 2. Ratio between the effective electronic mass, m^*, in presence of on-site Coulomb interaction U, and the mass m_b obtained from a LDA calculation.

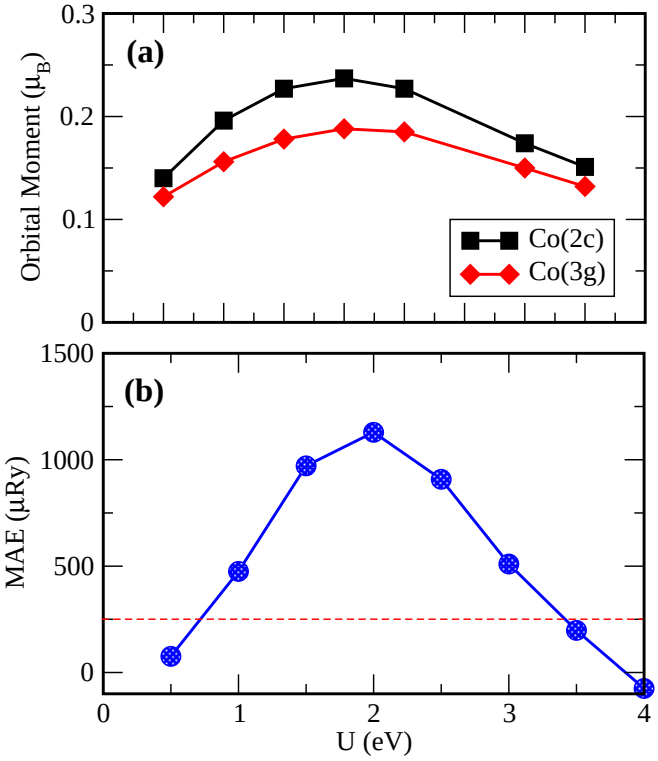

FIG. 3. On-site Coulomb U dependence of the orbital magnetic moments on Co sites and magnetocrystalline anisotropy energy (MAE) per formula unit of YCo_5. All the solid curves correspond to the results obtained with the LDA+DMFT method described in the text. The dashed line corresponds to the measured valued according to Ref. [31].

constructed with $4s$, $4p$, and $3d$ states for the Co atoms, and $5s$, $5p$, $4d$ for Y atoms. The N_k **k**-points are distributed with the conventional Monkhorst-Pack grid, and the Brillouin zone integration is carried out with the Fermi smearing at a temperature of $T = 474$ K. To explore the role of electronic correlation effects arising from the screened Coulomb interaction U, we fix the higher order slater integrals of $F^2 = 7.75$ eV, and $F^4 = 4.85$ eV from Ref. 29. These values of F^2 and F^4 for the d-orbitals result in a Stoner parameter $J = 0.9$ eV, which is consistent with the value used in earlier studies of Co metals [18]. We treat the effect of the Coulomb exchange interaction with F^2 and F^4 explicitly.

We first explore the relevance of the notion of electronic correlation in the ferromagnetic magnetic metals by studying the quasiparticle renormalization effect. In connection with the specific heat coefficient as measured from the thermodynamic experiments, the effective mass enhancement is proportional to the ratio of the quasiparticle density of states to band one at the Fermi energy: $m^*/m_b = \tilde{\rho}(E_F)/\rho_b(E_F)$. For the cases where the d electrons are active carriers, the band density of states has a predominant d-character: $\rho_b(E_F) = \sum_{i,\alpha} w_i \rho_{b,\alpha}(E_F)$, where $\rho_{b,i,\alpha}$ is the partial density of states at the Fermi energy from the 10 spin orbitals for the i-th type of Co atom. Here α is the spin-orbital index, while w_i is the number of equivalent atoms of a given type. Within a renormalized band theory, we can generalize the quasiparticle density of states at the Fermi energy as $\tilde{\rho}_b(E_F) = \sum_{i,\alpha} w_i \tilde{\rho}_{b,\alpha}(E_F)$. Here the spin-orbital dependent quasiparticle density of states at the Fermi energy is given by $\tilde{\rho}_{b,i,\alpha}(E_F) = \rho_{b,\alpha}(E_F)/z_{i,\alpha}$, where the quasiparticle weight is $z_{i,\alpha} = [1 - \partial \mathrm{Im}\Sigma_\alpha(i\omega_n)/\partial\omega_n|_{\omega_n \to 0}]^{-1}$ with the self-energy Σ_α defined on the Matsubara frequency ω_n axis.

Figure 2 shows the U dependence of the mass enhancement relative to LDA calculations, m^*/m_b, obtained by applying the LDA+DMFT method to YCo_5. We refer to the Methods section for technical details of this calculation. As expected, the effective mass increases monotonically with U. The mass enhancement takes values between 1.5 and 2 for U varying between 2.5 and 4 eV. The Sommerfeld coefficient γ of the specific heat is proportional to the effective mass of the quasiparticles. Based on our specific heat measurements of YCo_5, we obtain a Sommerfeld coefficient $\gamma = 90$ mJ/mol$\cdot$K$^2\cdot$f.u., which is ~ 2.7 times larger than the value $\gamma_b \simeq 33$ mJ/mol$\cdot$K$^2\cdot$f.u. extracted from pure LDA calculations (see Appendix **??**). Note that some additional contribution to the electronic renormalization arising from the electron-phonon coupling is not included in our calculations. Because γ/γ_b is equal to m^*/m_b, this ratio indicates that YCo_5 is a rather correlated metal for U between 2.5 and 4 eV. Values of U in this range have been previously reported in the YCo_5 literature [18, 29].

Fig. 3(a) shows the orbital magnetic moments on the two inequivalent Co atoms as a function of U. The orbital moment of the Co(2c) atoms is always larger than the moment of the Co(3g) atoms and both depend non-monotonically on U, reaching their maximum values at $U \simeq 2$ eV. The results for $U \to 0$ reproduce the values obtained in previous LDA calculations [7, 13], while the moments increase by a factor of ~ 2 for $U \simeq 1-3$ eV. This increase is consistent with our XMCD measure-

ments, which indicate that the average orbital magnetic moment on the Co ion is 0.20 μ_B. This observation confirms the relevant role of U on the formation of a strong orbital moment.

However, the most dramatic effect of the on-site Coulomb repulsion U appears when we compute the MAE, as is clear from our LDA+DMFT results shown in Fig. 3(b). By comparing Figs. 3(a) and (b), we can see that the MAE and the size of the orbital moments exhibit the same non-monotonic dependence on U. The extrapolated LDA value of the MAE is much lower than the measured value of $K_1V = 250$ μRy shown with a dashed line in Fig. 3 (b) ($V = 0.84 \times 10^{-22}$ cm^3 is the volume of the primitive unit cell and $K_1 = 2.98 \times 10^{18}$ Ry/cm^3 [31]). *However, the MAE increases drastically with U reaching values that are more than an order of magnitude higher in the range U* ∼1-3.5 eV. This dramatic increase not only explains the reason why LDA calculations systematically underestimate the MAE of strong magnets, but also shows the crucial role played by electronic correlations in the development of large magnetic coercivity. In addition, the MAE obtained from our LDA+DMFT calculations for U between 3 and 3.5 eV is in good agreement with the experimental value.

V. CONCLUSIONS

The fact that the strongest magnets are rare-earth based compounds, suggests that the large magnitude of the SO coupling plays a crucial role in the development of high coercivity. One would then expect that the intrinsic magnetocrystalline anisotropy of $Nd_2Fe_{14}B$ or $SmCo_5$ originates in the crystal field splitting of the rare-earth $4f$ levels. There is experimental evidence, however, indicating that substantial magnetocrystalline anisotropy may be associated with the transitional metal sublattice itself. For instance, the coercive field of magnetically hardened $Gd_2Fe_{14}B$ is 2.5 kOe [32, 33], but the Gd^{3+} ion has no orbital moment. In addition, the MAE of $SmCo_5$ is only three times higher than the MAE of YCo_5 and Y is non-magnetic. Our results indicate that the MAE of a magnet is dramatically modified by the presence of strong on-site Coulomb interaction U that tends to localize the electrons. We note that enhanced correlations could also be playing a role in rare-earth based compounds (rare-earths have large ionic radii). This may explain why rare-earth based compounds, in which the rare-earth has no orbital moment, still have very high MAE.

By a close comparison of our LDA+DMFT calculations with different key experimental measurements, we have shown that electronic correlation effects play an essential role in determining the MAE of YCo_5. These calculations suggest that the figure of merit of strong magnets can be greatly optimized by tuning the electron Coulomb repulsion U. Our analysis has natural implications for the search of rare-earth free strong magnets. While it may be important to retain a large SO coupling, it is equally or even more important to find strongly correlated ferromagnets in order to induce a large enough orbital moment on the transition metal. Consequently, a relevant guiding principle in the search for rare-earth free strong magnets is to find Fe or Co rich structures with narrow $3d$ bands.

ACKNOWLEDGMENTS

We are grateful to Tomasz Durakiewicz, O. Gränäs, J. Schweizer, F. Tasset, P. Thunström, and J. M. Wills for helpful discussions. Work at the LANL was performed under the auspices of the U.S. DOE contract No. DE-AC52-06NA25396 through the LDRD program. Part of the theoretical calculations were carried out on a Linux cluster in the Center for Integrated Nanotechnologies, a DOE Office of Basic Energy Sciences user facility.

Appendix A: Specific Heat Measurements on YCo_5

We perform the specific heat measurements on polycrystalline samples of YCo_5, which were made by arc-melting the constituents on a water-cooled copper hearth. It was measured down to 2 K in zero magnetic field using a thermal relaxation method implemented in a Quantum Design PPMS-9 device. The data is shown in Fig. 4. The Sommerfeld coefficient (γ) was found to be 90 mJ/mol·K^2 by fitting C/T below 10 K to the form of $\gamma + \beta T^2 + \delta T^4$. We attribute γ to the electronic contribution to the heat capacity, while the lattice and magnetic contributions are accounted for by the βT^2 and δT^4 terms.

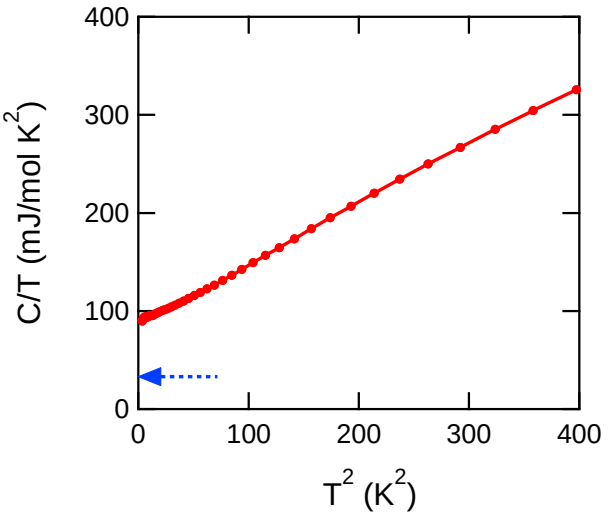

FIG. 4. (Color online) C/T vs T^2 for YCo_5, from which we obtain the Sommerfeld coefficient γ in the $T \to 0$ limit. The dashed arrow is value expected based on the band calculations.

To obtain the mass enhancement due to strong corre-

lations we compare the measured Sommerfeld coefficient to the bare density of states obtained by our DFT calculations using the generalized gradient approximation with the Perdew-Burke-Ernzerhof exchange correlation potential [36]. Both the full-potential linear muffin-tin orbital method as implemented in the RSPt [30] program and the full-potential linearized augmented plane wave as implemented in Wien2k [37] program give the consistent results. By summing both spin contributions we find the density of states at the Fermi level $N(E_F) = 14$ states/eV. From this we obtain a mass enhancement $m^*/m_b = \gamma/(\pi^2 k_B^2 N(E_F)/3) = 2.7$.

Appendix B: X-ray Circular Magnetic Dichroism measurements on YCo_5

The XMCD measurements were carried out in a total electron yield detection scheme at the beam line 4-ID-C of the Advanced Photon Source, Argonne National Laboratory. The beamline 4-ID-C has the ability to generate circularly polarized x-rays at the resonances of 3*d* elements with high degree of circular polarization ($> 97\%$) by means of an electromagnetic circularly polarizing undulator, including the ability to switch polarization state with a 1 Hz frequency. For the XMCD measurements the samples have been ground into fine powder and been pressed directly into electrically conducting carbon tape and placed in contact with a Cu holder. The Cu holder was electrically isolated from the cold finger by a sapphire disk. The samples were placed into a 7 Tesla superconducting magnet with a variable temperature insert. All scans were carried out at a temperature $T = 20$ K and over an energy range of 770 to 810 eV to measure the Co L_3- and L_2-edges (778.1 and 793.2 eV, respectively). Total electron yield data sets μ^+ and μ^- recorded with left- and right-circularly polarized x-rays, respectively, were background subtracted and edge-step normalized (edge is normalized to one). Moreover, each measurement was carried out for magnetic fields $H = 6$ Tesla directed along and opposite to the photon wave vector, respectively, to check for experimental artifacts. Using μ^+ and μ^- the normalized XANES ($\mu_0 = \frac{\mu^+ + \mu^-}{2}$) and XMCD ($\Delta\mu = \mu^+ - \mu^-$) data sets for YCo_5 were obtained. The orbital contribution to the magnetic moment was then extracted using the sum rules for 3*d* transition metals [34, 35]:

$$L = -\frac{4}{3} n_h \frac{\Delta I_{L_3} + \Delta I_{L_2}}{I_{L_3} + I_{L_2}}, \tag{B1}$$

where n_h is the number of holes in the 3*d* shell, and $n_h = 3$ for the $3d^7$ configuration of Co in YCo_5. I_{L_2}/I_{L_3} are the integrated intensity in the isotropic white lines at the L_2/L_3 edges, and $\Delta I_{L_2}/\Delta I_{L_3}$ are the integrated intensities in the partial dichroic signal.

[1] L. Lewis and F. Jimnez-Villacorta, *Perspectives on permanent magnetic materials for energy conversion and power generation*, Metall. Mater. Trans. **A 44**, 2 (2013).

[2] H. R. Kirchmayr and C. A. Poldy, *Handbook on the Physics and Chemistry of Rare Earths*, Lecture Notes in Physics, Vol. 2 (North.Holland, Amsterdam, 1979).

[3] F. Bloch and G. Gentile, *Zur Anisotropie der Magnetisierung ferromagnetischer Einkristalle*, Z. Phys. **70**, 395 (1931).

[4] H. Brooks, *Ferromagnetic anisotropy and the itinerant electron model*, Phys. Rev. **58**, 909 (1940).

[5] G. H. O. Daalderop, P. J. Kelly, and M. F. H. Schuurmans, *First-principles calculation of the magnetocrystalline anisotropy energy of iron, cobalt, and nickel*, Phys. Rev. B **41**, 11919 (1990).

[6] H. J. F. Jansen, *Origin of orbital momentum and magnetic anisotropy in transition metals*, J. Appl. Phys. **67**, 4555 (1990).

[7] L. Nordstrom, M. S. S. Brooks, and B. Johansson, *Calculation of orbital magnetism and magnetocrystalline anisotropy energy in YCo_5*, J. Phys.: Condens. Matter **4**, 3261 (1992).

[8] J. Schweizer and F. Tasset, *Polarised neutron study of the RCo_5 intermetallic compounds. I. The cobalt magnetisation in YCo_5*, J. Phys. F: Metal Physics **10**, 2799 (1980).

[9] A. Heidemann, D. Richter, and K. H. J. Buschow, *Investigation of the hyperfine fields in the compounds $LaCo_{13}$, $LaCo_5$, YCo_5 and $ThCo_5$ by means of inelastic neutron scattering*, Z. Phys. B **22**, 367 (1975).

[10] M. Brooks, *Calculated ground state properties of light actinide metals and their compounds*, Physica B+C **130**, 6 (1985).

[11] O. Eriksson, M. S. S. Brooks, and B. Johansson, *Orbital polarization in narrow-band systems: Application to volume collapses in light lanthanides*, Phys. Rev. B **41**, 7311 (1990).

[12] J. Alameda, J. Deportes, and D. Givord, R. Lemaire, and Q. Lu, *Large magnetization anisotropy in uniaxial YCo_5 intermetallic*, J. Magn. Magn. Mater. **1518**, Part 3, 1257 (1980).

[13] H. Takahashi, S. Ohtsuka, T. Ukai, and N. Mori, *On the orbital moment of Co in YCo_5*, J. Magn. Magn. Mater. **70**, 189 (1987).

[14] J. B. Goodenough, *Magnetism and the Chemical Bond* (Interscience-Wiley, New York, 1963).

[15] I. Yang, S. Y. Savrasov, and G. Kotliar, *Importance of correlation effects on magnetic anisotropy in Fe and Ni*, Phys. Rev. Lett. **87**, 216405 (2001).

[16] G. Kotliar, S. Y. Savrasov, K. Haule, V. S. Oudovenko, O. Parcollet, and C. A. Marianetti, *Electronic structure calculations with dynamical mean-field theory*, Rev. Mod. Phys. **78**, 865 (2006).

[17] M. E. Pezzoli, K. Haule, and G. Kotliar, *Neutron magnetic form factor in strongly correlated materials*, Phys. Rev. Lett. **106**, 016403 (2011).

[18] A. Grechnev, I. Di Marco, M. I. Katsnelson, A. I. Lichtenstein, J. Wills, and O. Eriksson, *Theory of bulk and surface quasiparticle spectra for Fe, Co, and Ni*, Phys. Rev. B **76**, 035107 (2007).

[19] R. M. Martin, *Electronic Structure: Basic theory and practical methods* (Cambridge University Press, Cambridge, 2004).

[20] R. D. Cowan, *The Theory of Atomic Structure and Spectra* (University of California Press, Berkeley, 1981).

[21] M. Czyzyk, G. Sawatzky, *Local-density functional and on-site correlations: The electronic structure of La_2CuO_4 and $LaCuO_3$*, Phys. Rev. B **49**, 14211 (1994).

[22] J. H. Shim, K. Haule, and G. Kotliar, *Fluctuating valence in a correlated solid and the anomalous properties of δ-plutonium*, Nature **446**, 513-516 (2007).

[23] J.-X. Zhu, R. C. Albers, K. Haule, G. Kotliar, and J. M. Wills, *Site-selective electronic correlation in α-plutonium metal*, Nat. Commun. **4**, 2644 (2013).

[24] V. I. Anisimov, A. I. Poteryaev, M. A. Korotin, A. O. Anokhin, and G. Kotliar, *First-principles calculations of the electronic structure and spectra of strongly correlated systems: dynamical mean-field theory*, J. Phys.: Condens. Matter **9**, 7359 (1997).

[25] L. Craco, M. S. Laad, S. Leoni, and E. Müller-Hartmann, *Insulator-metal transition in the doped $3d^1$ transition metal oxide $LaTiO_3$*, Phys. Rev. B **70**, 195116 (2004).

[26] K. Held, G. Keller, V. Eyert, D. Vollhardt, and V. I. Anisimov, *Mott+Hubbard Metal-Insulator transition in paramagnetic V_2O_3: An LDA+DMFT(QNC) study*, Phys. Rev. Lett. **86**, 5345 (2001).

[27] M. S. Laad, L. Craco, and E. Müller-Hartmann, *Orbital switching and the first-order insulator-metal transition in paramagnetic V_2O_3*, Phys. Rev. Lett. **91**, 156402 (2003).

[28] L. V. Pourovskii, M. I. Katsnelson, A. I. Lichtenstein, *Correlation effects in electronic structure of actinide monochalcogenides*, Phys. Rev. B **72**, 115106 (2005).

[29] O. Granas, I. Di Marco, P. Thunstrom, L. Nordstrom, O. Eriksson, T. Bjorkman, and J. M. Wills, *Charge self-consistent dynamical mean-field theory based on the full-potential linear muffin-tin orbital method: Methodology and applications*, J. Comput. Mat. Sci. **55**, 295 (2012).

[30] J. M. Wills, O. Eriksson, M. Alouani, and D. L. Price, eds., *Full-Potential Electronic Structure Method: Energy and Force Calculations with Density Functional and Dynamical Mean Field Theory* (Springer-Verlag, Berlin, 2010).

[31] R. Skomski and J. M. D. Coey, eds., *Permanent Magnetism* (Taylor and Francis Group, Oxon, Great Britain, 1999).

[32] J. F. Herbst, J. J. Croat, F. E. Pinkerton, and W. B. Yelon, *Relationships between crystal structure and magnetic properties in $Nd_2Fe_{14}B$*, Phys. Rev. B **29**, 4176 (1984).

[33] J. J. Croat, J. F. Herbst, R. W. Lee, and F. E. Pinkerton, *PrFe and NdFe based materials: A new class of high performance permanent magnets (invited)*, J. Appl. Phys. **55** (1984).

[34] B. T. Thole, P. Carra, F. Sette, and G. van der Lann, *X-Ray Circular Dichroism as a Probe of Orbital Magnetization*, Phys. Rev. Lett. **68**, 1943 (1992).

[35] P. Carra, B. T. Thole, M. Altarelli, and X. Wang, *X-Ray Circular Dichroism and Local Magnetic Fields*, Phys. Rev. Lett. **70**, 694 (1993).

[36] J. P. Perdew, K. Burke, and M. Ernzerhof, *Generalized Gradient Approximation Made Simple*, Phys. Rev. Lett. **77**, 3865 (1996).

[37] P. Blaha, K. Schwarz, G. K. H. Madsen, D. Kvasnicka, and J. Luitz, *WIEN2k: An Augmented Plane Wave + Local Orbitals Program for Calculating Crystal Properties* (Tech. Universitat Wien, Austria, 2001).